

An Integrated Open-Cavity System for Magnetic Bead Separation and Manipulation

Faisal T. Abu-Nimeh and Fathi M. Salem

Abstract—Superparamagnetic beads are generally used in biomedical assays to manipulate, maneuver, separate, and transport bio-materials. We present a low-cost integrated system designed in bulk $0.5\mu\text{m}$ process to automate the manipulation and separation process of magnetic beads. The system consists of an 8×8 coil-array suitable for a single bead manipulation, or collaborative manipulation using pseudo-parallel executions. The size of a single coil is $30\mu\text{m} \times 30\mu\text{m}$ and the driver DC current source supports 8 different levels up to 1.5mA. The total power consumption of the entire system is 9mW when running at full power and it occupies an area of $248\mu\text{m} \times 248\mu\text{m}$.

I. INTRODUCTION

Low cost lab-on-chip platforms are establishing a new venue for clinical diagnostics specifically in point-of-care testing (POCT) and in-field deployment. They are becoming more attractive due to their portability, inexpensiveness, disposability, robustness, reliability, and high throughput. By using very small sample volumes (in the order of $1\text{-}100\mu\text{L}$) one can identify, diagnose, or separate samples with very high precision using superparamagnetic beads.

Binding bio-materials to magnetic beads is relatively simple. It requires a standard preparation protocol which depends on the surface coating of the bead. Manufacturers offer variety of coatings to enable easier binding and faster deployment. For further discussion on the use of magnetic beads in analyzing biological and chemical samples, the reader is referred to a recent review by M. Gijs et al. [1].

Current state-of-the-art requires [1]–[4] either capillaries or microfluidic channels and pumps to guide the samples into chambers or fenced regions for manipulation and sensing. On the other hand, [5] use mechanical structures such as spin valve arrays where the magnetic bead can be sensed/trapped, or use micro-magnetic-tweezers [6] to guide a bead to a pre-defined path.

In [7], we have introduced the ability to manipulate and sense magnetic beads in the order of $1\mu\text{m}$ using AC currents for manipulation, RF oscillators for sensing, and an open-cavity device to eliminate microfluidic structures and pumps for low-cost packaging. In this work, we expand on and complement the previous efforts by introducing (i) a new programmable manipulation scheme using DC currents and more powerful forces (ii) a closely stacked array design

for singular manipulation and collaborative pseudo-parallel transportation of larger biological objects, and (iii) a new packaging for faster testing and deployment. For an overview of the methodology and proposed control for these systems refer to [8] for some of the challenges and benefits.

The paper is organized into four sections. In section II, the overall system design and integration is introduced, followed by a description and validation of each component used. Next, section III includes the general electrical and physical characterization of the IC fabrication, packaging, general isolation techniques, and tests. Finally, the conclusion is in section IV.

II. SYSTEM INTEGRATION

We present the design of an 8×8 magnetic manipulation coil-array fabricated in standard $0.5\mu\text{m}$ CMOS, suitable for bio-medical applications. The size of the array is in the order of $248\mu\text{m} \times 248\mu\text{m}$ and a single coil occupies $30\mu\text{m} \times 30\mu\text{m}$. The spacing between any two coils is $0.9\mu\text{m}$, which is the smallest DRC (Design Rule Checking) value permissible in this CMOS technology. As a result of stacking the coils of the array closely, by moving digital switches and controllers to the sides, one can build an arbitrary number of magnetic field forces using collaborative actuation across the array. The system-level block diagram depicted in figure 1 consists of four major components; the 8×8 coil array, 3-to-8 row and column decoders, a variable power bi-directional current source, and the global control. First, the global control is responsible for: (a) coordinating the magnetic fields generated by providing the correct signals to the decoders and the current source, (b) providing a flexible interface to allow programmable off-chip algorithms for control and manipulation, (c) fast switching with a period of 25n seconds for pseudo-parallel collaborative or single-coil manipulation. Second, the row/column decoders and digital logic (a) facilitate single coil selection (b) minimize interconnect coupling and noise and (c) lower the overall number of I/O pins of the package. Third, an eight-level bi-directional current source to generate different magnetic flux densities and directions for refined maneuvering. Last component is the actual coil-array where electric current is passed through a pre-selected coil location to generate an electromagnetic field using on-chip multi-layered inductors.

The following subsections describe each component's functionality with supportive simulations:

F. T. Abu-Nimeh is a Ph.D candidate at the department of Electrical and Computer Engineering, Michigan State University, East Lansing, MI, 48824, USA asdl815@egr.msu.edu

F. M. Salem is a Professor at the department of Electrical and Computer Engineering, Michigan State University, East Lansing, MI, 48824, USA salem@egr.msu.edu

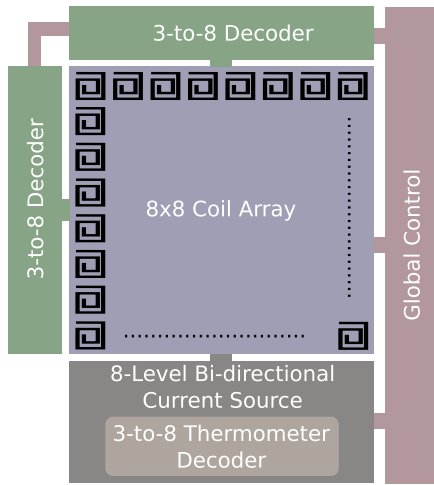


Fig. 1. System-level block diagram.

A. Programmable Current Source

NMOS transistors are used to sink currents through a coil. The resistance of the path (including the coil) as well as the width/length of the transistor set the amount of current which can be sunk, thus, eliminating the need for a dedicated resistor to set a reference current. However, the maximum current drawn has to heedfully confront with the technology's current density limits in order to keep the substrate at room temperature and protect the metal layers and the oxide from melting.

We cascaded a set of eight NMOS transistors in parallel to create a binary controllable current sink. A simplified depiction of this configuration is shown in figure 2. It operates as follows: a user selects a single coil from the 8x8 array using *row* and *column* signals. Next, the direction (polarity) of the current is selected (e.g. counter-clockwise or clockwise) using S and \bar{S} . The parallel NMOS block as well as the current direction (polarity) switches are shared across the whole array to reduce real-estate. An eight bit word $en[0:7]$ is used to adjust the amount of current required for actuation. Figure 3 shows a post-layout, with parasitic capacitance and resistance extracted, simulation of the programmable current sink. When the signal S is high the direction of the current is positive (counter-clockwise for the spiral coil) and vice versa. The non-linearity of the steps are a result of the parallel NMOS arrangement, however, if real-estate is sparse one can create better sources/sinks with more complex circuits.

B. Digital Logic

To individually access each coil in the 8x8 array two 3-to-8 decoders link any inductor load to the programmable current source. The decoders operate as in Random Access Memory (RAM), each input enables one of the eight rows or columns available. For pseudo-parallel manipulation schemes a high-speed control signal (switching at 40 MHz) is used to link a specific cell to the driving circuitry and it consists of a dedicated transmission gate as well a AND gate [7].

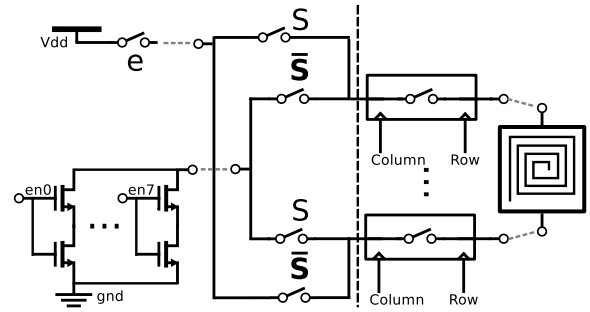


Fig. 2. Variable power bi-directional current sink with a simplified coil path. The 'e' signal is an "enable" signal which can be used to switch on/off the entire DC actuation path. The components on the right of the dashed line are shared across the entire array to save area.

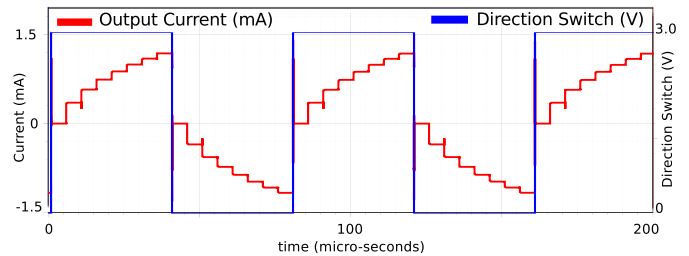


Fig. 3. Post-layout simulation of one of the programmable current sources implemented on chip. The magnetic field direction can be changed using the positive current stairs or the negative ones.

C. Actuator Array

To target larger forces (up to 6nN) a larger on-chip coil actuator is designed. A square shape spiraling inductor is selected in this design to meet "Non-Manhattan-shape" DRC rule in this CMOS technology. All coils in the array are similar and have the following characteristics: its resistance is 23.94 Ohms, its DC inductance is 1.125 nH, its length is 30 μ m, the metal track width is 1.8 μ m, the spacing between traces is 1.2 μ m, and the number of turns is 5. To measure the force and the magnetic flux density generated from this coil we used a Finite-Element-Method (FEM) simulator. By precisely modeling the CMOS substrate, metal layers, and passivation layers, using the process' proprietary specifications, we receive the most accurate results as shown in figure 4. The X-Axis represents the distance from the center of the 30 μ m x 30 μ m coil, the Y-Axis is the magnitude of the magnetic flux density (B). The generated field near the coil the center will have two maxima due to the fact that the coil is not a perfect spiral (a square in our case). As the distance increases this effect becomes less dominant. Therefore, to lessen having two maxima, one can apply a 2 μ m silicon oxide and silicon nitride layers which also serves as a protection layer for the platform.

To measure the forces acting on the bead, we used different Invitrogen DYNAL®magnetic bead sizes which were modeled using the physical specifications as well as the B-H hysteresis curves provided by the manufacturer. As a result, when a current of 1.5mA is passed through the coil, the force (6.0354nN) acting on the surface of the bead is

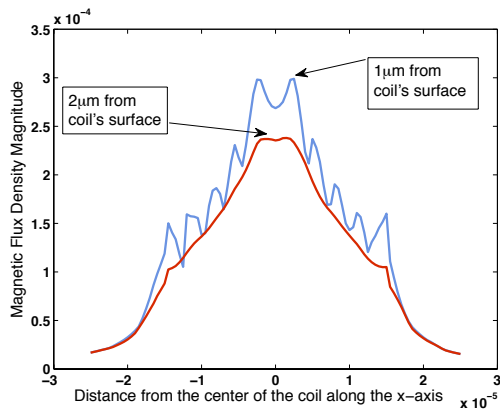


Fig. 4. FEM simulation of the magnetic flux density at the surface of the chip and near the metal spiral, without the bead.

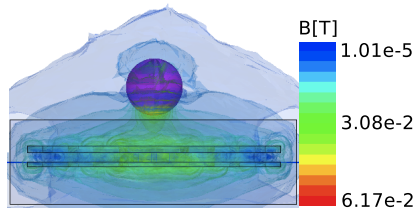


Fig. 5. Side view of the coil's magnetic flux density while passing a 1.5mA current through it with a bead centered on top. The force reported by the simulator acting on the bead at the surface is 6nN.

calculated by the virtual work method using the magnetic flux density as shown in figure 5. The blue color represents the weakest and the red color is the strongest magnetic field level. The magnetic coupling between the coil and the bead causes the magnetic field generated by the coil to be more focused toward the center of the sphere.

The present CMOS technology we used supports three metal layers. Therefore, the upper most two metal layers are used to create the coil and the lower most layer is used for routing (e.g. interconnecting the coil's two ports to their corresponding switches). Careful routing techniques are required to (a) minimize the coupling across interconnects (b) accommodate the largest number of coils in the array while keeping the distance between any two coils the minimalist e.g. $0.9\mu\text{m}$ (c) shorten the routing path to keep the interconnect resistance minimum.

D. Global Control

The 25ns switching period allows us to share the same driving circuitry to manipulate smaller objects in the order of $1\mu\text{m}$ using a single coil, or larger objects in a pseudo-parallel execution using the entire array. To select a single coil the global control supplies three binary digits for the row, three binary digits for the column. There are 8 levels of actuation, a thermometer decoder is used to minimize the number of I/O's where the smallest input "000" translates to "0000 0001" and the largest input "111" translates to "1111 1111". The polarity of the field can be adjusted using a single bit where "0" is used for "pulling" and "1" is use for "pushing".

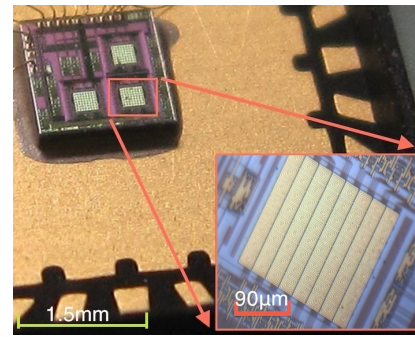


Fig. 6. Photograph of 1.5mm x 1.5mm CMOS die as an open cavity device.

Initially the magnetic bead is assumed to have a random magnetic moment, after being exposed to a constant field it acquires a new moment. The time constant of this process is in the millisecond range [2]. Therefore, one can "push" or "pull" the bead as long as it has a constant magnetic moment. Since the switching speed (25ns) is far smaller than the time constant of the bead it is assumed that the bead would not acquire a new moment (e.g. has a constant magnetic moment) during this operation.

III. RESULTS AND FUTURE WORK

Integrating all modules together on the same die requires careful examination in terms of routing, isolation, and coupling among neighboring coils. Moreover, the modular design should consider distributing heat equally across the entire array to maintain consistent interactions with the bio-objects of interest. The system, shown in figure 6, has three different 8×8 arrays; each one uses different routing and isolation techniques, DC driving circuitry, and configuration. The shape of the array can be adjusted as per the application of interest. Additionally, with different array design shapes, one can create an unlimited number collective 3D scenarios for manipulation. For example, using this square array one can program the global controller to set the center of the array on maximum power '111' and reduce the power along the X and Y axes in a gradient manner towards the edges to create a pyramidal field shape. The prototype arrays are fabricated in $0.5\mu\text{m}$ 3-Metal-2-Poly CMOS. It consumes 9mW using a 5v power supply. We used the $1.5\text{mm} \times 1.5\text{mm}$ die to fill it up with three 8×8 arrays. Each coil array occupies $248\mu\text{m} \times 248\mu\text{m}$ and requires a $100\mu\text{m} \times 260\mu\text{m}$ digital overhead (switches, decoders, etc).

A. Packaging

All of the components above except the external global control were integrated on the same die and fabricated using standard CMOS technology then packaged using standard plastic packages. Contrary to other state-of-the-art implementations, our method doesn't need any special post-processing such as microfluidic structures to channel or manipulate bio-materials. It is designed to operate as an "open cavity" device where the entire surface of the chip is exposed to the sample or material of interest. This reduces the complexity

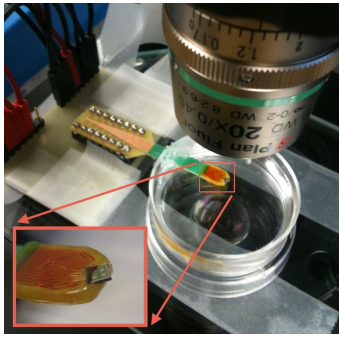


Fig. 7. Packaging of the CMOS die on top of a PCB probe.

of the system, makes it cheaper to manufacture, and more portable by eliminating microfluidic structures overhead and the micro-pumps associated with them. However, it introduces new challenges, in which, some are shared with microfluidics. The challenges are mainly in terms of packaging: insulating the wire bonds attaching the CMOS die with the ceramic/plastic package, biocompatibility of the surface of the die, and maneuvering the sample of interest on an open surface.

To validate and test the functionality of the design under the Microscope, a printed circuit board (PCB) is used to mount the CMOS die on the edge of an NeuroNexus A-series probe as in figure 7. The bonding wires are protected using EpoxyTechnology 353 ND and 353 NDT. The three on-chip arrays are exposed and submerged in Phosphate buffered saline (PBS) solution inside a Corning dish. Then small droplets of magnetic beads are applied on the surface of the chip.

B. Experiments

A lab experiment is conducted to validate the transport forces acting on a single bead in the X-Y plane. The setup is very similar to the one shown in figure 7. While the coils are switched off, small droplets ($5\mu\text{L}$) of a diluted magnetic beads solution are inserted in the PBS solution using a pipette. Then a small (1 minute) grace period is observed in order for the beads to settle in the fluid or on the surface of the chip. Using the Microscope, the user visually locates a magnetic bead on the 8×8 array and programs a specific coil to switch on to attract the bead towards it. Figure 8 shows multiple frames taken from a video sequence while a bead is being manipulated to the right. Initially (frames 1 and 2), the magnetic bead is far from the surface of chip, thus, out of focus. In frames 3, 4, and 5 the bead is attracted closer to the surface by switching on the coil on the left. Finally, in the remaining frames the bead is transported to the right by switching off the coil on the left and switching on the coil on the right. The bead didn't move to the center of the coil due to several possible factors: The X-Y transitional forces are not strong enough to influence the bead, the bead found a preferred binding site and attached itself to it, or the equilibrium forces acting on the bead are not maximized at the center of the coil (this is caused by the fact that the

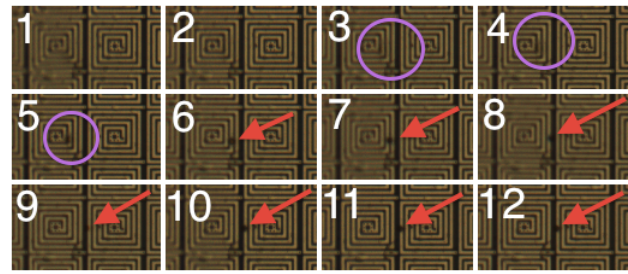


Fig. 8. A montage of a series of video frames showing how a magnetic bead is attracted (downward) toward a coil then move to the right by switching on the neighboring coil.

main vdd-rail, which is exposed, is contributing to the the transition; careful vdd-gnd shielding is required to alleviate this influence). The total distance traveled in this experiment is $16\mu\text{m}$ in 3.3 seconds.

C. Future Work

For future implementations, larger coils, larger amounts of DC currents, and interconnect shielding are planned. Additionally, an autonomous on-chip control algorithm can be developed to automate the manipulation process and make it more robust for biomedical applications.

IV. CONCLUSION

An open cavity device designed in bulk $0.5\mu\text{m}$ CMOS technology capable of creating forces up to 6nN in order to manipulate and separate superparamagnetic beads bound to biological and chemical materials. The system consumes 9mW when running at full capacity at room temperature using three $248\mu\text{m} \times 248\mu\text{m}$ coil arrays. Each coil measures $30\mu\text{m} \times 30\mu\text{m}$ in the X-Y plane. The coil array can be controlled individually for singular bead manipulation or collaboratively in pseudo-parallel fashion for larger objects.

REFERENCES

- [1] M. Gijs, F. Lacharme, and U. Lehmann, "Microfluidic applications of magnetic particles for biological analysis and catalysis," *Chemical Reviews*, vol. 110, no. 3, pp. 1518–1563, Mar 2010.
- [2] H. Lee, Y. Liu, D. Ham, and R. Westervelt, "Integrated cell manipulation system—cmos/microfluidic hybrid," *Lab on a Chip*, vol. 7, no. 3, pp. 331–337, 2007.
- [3] Y. Moser, T. Lehnert, and M. Gijs, "On-chip immuno-agglutination assay with analyte capture by dynamic manipulation of superparamagnetic beads," *Lab on a Chip*, Jan 2009.
- [4] U. Lehmann, M. Sergio, E. Dupont, and E. Labonne, "Actuation and detection of magnetic microparticles in a bioanalytical microsystem with integrated cmos chip," *Nanosystems Design and Technology*, Jan 2009.
- [5] W. Altman, J. Moreland, S. Russek, and V. Bright, "Optimization of spin-valve parameters for magnetic bead trapping and manipulation," *Journal of Magnetism and Magnetic Materials*, vol. 322, no. 21, pp. 3236–3239, 2010.
- [6] Z. Zhang, Y. Huang, and C.-H. Menq, "Actively controlled manipulation of a magnetic microbead using quadrupole magnetic tweezers," *Robotics, IEEE Transactions on*, vol. 26, no. 3, pp. 531 – 541, 2010.
- [7] F. Abu-Nimeh and F. Salem, "Integrated magnetic array for bio-object sensing and manipulation," *Biomedical Circuits and Systems Conference (BioCAS), 2010 IEEE*, pp. 62 –65, Nov 2010.
- [8] F. Abu-Nimeh and F. Salem, "Electro-magnetic sensing and actuation array on silicon substrate platforms," *Nanotechnology Materials and Devices Conference (NMDC), 2010 IEEE*, pp. 119–122, Oct 2010.